Torque-speed Curve of Dc Braking Induction Motors Including Saturation Effect

Pichai Aree* and Nakarin Prempri

Power System and Machine Research Group

Department of Electrical Engineering, Thammasat University, Pathumthani, Thailand ,

Abstract

Induction motors are widely used in industrial application. Often, braking is necessary to stop their operations in cases of emergency. One of the simple braking methods is d.c. injection current. In order to stop the motors in efficient manner, their accurate speed-torque curves in the braking zone are often required. Thus, in this paper, effects of nonlinear saturation and variation in the rotor resistance on torque-speed curves are further investigated. The measured and calculated torque-speed curves are compared for validation. The study result shows a good agreement of the torque-speed curves between measurement and calculation in the satisfactory manner when the saturation effects in both mutual and rotor-leakage reactances as well as slip-dependent rotor resistance are fully taken into account.

Keyword: Induction Motor; Braking; dc injection current; Torque-speed curve

1. Introduction

Three-phase induction motors are widely used in most industrial process. Often getting them to stop is very much required for emergency situation [1]. Hence, braking plays an important role to stop the induction motors. Besides mechanical brakes, electric braking can be employed to give a more immediate stop because it is fast and effective with less running cost. Electrical braking can be done by different ways: plugging braking, regenerative braking, dynamic braking [2] . The plugging method gives the fastest stop but it can be harsh on electrical and mechanical components. The regenerative braking is used to decelerate the motor rather than bring it to a complete stop [3]. Often, the back-up braking such as d.c. dynamic braking is required to slow the motor at low speeds. For dynamic braking, the a.c. power supply must be disconnected. The stator of a running induction motor is then connected to d.c. supply. So, a stationery magnetic field produced by the d. c. current flow induces rotor current flowing in the moving rotor winding [4]. The machine works a generator in which the generated energy is dissipated in the rotor resistance. This process produces a braking torque to bring the rotor to rest quickly.

In order to stop the induction motors in more efficient manner, their torque-speed curves under d.c. current injection is often needed to be known [5] . For example, the accurate torque-speed curve is mostly required for evaluating the braking time of induction motors. Commonly, the torque-speed curves of induction motors can be calculated using a well-known steady-state equivalent circuit [6]. Because high d.c. current can be injected into the motors up to three times of its full-load ampere. The saturation may affect in the motor braking torque performance [7]. Moreover, since the motor is brought to rest from the rated speed, a great variation in rotor frequency from the rated value to zero is more noticeable. In this case, the skin effect in rotor bars may introduce a great change on the rotor equivalent resistance, affecting the torque- curve characteristics [8].

Based on the literature review, the nonlinear effects in saturation and variation in rotor resistance of induction motor are often ignored in most study of d.c. injection braking. Thus, in this paper, the torque-speed curves of

* Corresponding author. Tel.: +66896711678

E-mail address: apichai@engr.tu.ac.th

induction motors under d.c. braking are fully incorporated with the nonlinear effects. The saturation of mutual and rotor-leakage reactances are taken into account as well as the slip-dependent rotor resistance. The experimental study is conducted for verification.

2. Torque-speed curve of induction motor under braking

In order to compute the torque curve of motor under d.c. current injection, the common equivalent circuit of induction motor is employed [9]. For simplicity, the stator resistance is ignored. Because the stator leakage reactance is zero due to making use of d.c. current, the motor equivalent circuit can be modified as shown in Fig. 1

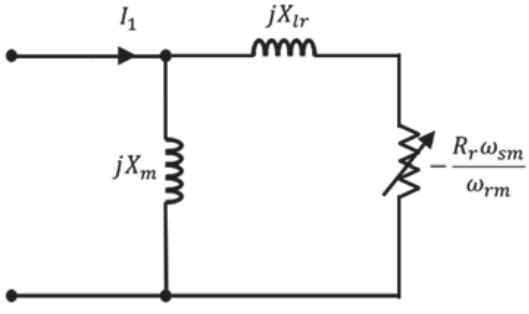

Fig. 1. Equivalent circuit of induction motor under d.c. braking

According to the circuit in Fig. 1, X_m and X_{lr} are mutual and rotor-leakage reactance. I_1 is stator resultant current per phase. ω_m and ω_{rm} are synchronous and rotor angular velocity in mechanical degree. Referred to Fig. 1, the braking torque of induction motor can be written by,

$$Te = \frac{-I_1^2 X_m^2 R_r / \omega_{rm}}{\left(R_r\omega_{sm} / \omega_{rm}\right)^2 + (X_{lr} + X_m)^2)} \qquad (1)$$

3. Test system

In order measure the torque-speed curve, the test system shown in Fig. 2 is used. It consists of Y- connected induction motor rated 1kW, 400V, 2.8A, 1420 rpm. The motor is directly coupled to a larger motor drive (4kW induction motor) via a torque sensor. The motor speed is measured using the tachometer attached on the same shaft. The input stator current is also detected using hall-effect sensors. Torque, speed, and current signals are then delivered to data acquisition card, interfaced with LabVIEW software. During the experiment, the test motor (1kW) is energized by direct-on-line method. Once the motor reaches rated speed, the a.c. power supply is disconnected. The d.c. supply is immediately injected. At this time, the motor drive controlled by inverter in the ramp down mode is employed to control speed of the test motor from no-load speed up to zero. The torque and speed signals are recorded with sampling frequency of 20k samples/sec and displayed in the computer. After that, the noise reductions in the recorded torque and speed signals are performed by the smoothing operation using moving average filters.

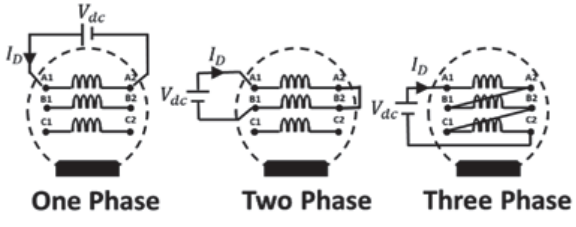

2a Three different configurations of test motor during d.c. injection

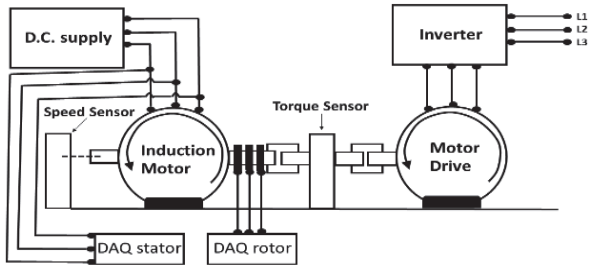

2b test bench

Fig. 2. The test system

4. Determination of motor parameters

This section explains how to obtain the key parameters of induction motors for computing the braking torque curve. A novel method based on d.c. excitation technique is employed in order to measure only the magnetizing inductance of the motors (without including the effect of stator leakage inductance). During the experiment, the d.c. current is energized into one of the three phase windings, while the induced e.m.f. is directly measured from the other remaining phase. The profiles of the measured e.m.f. at different levels of currents (2A, 4A and 6A) are plotted as shown in Fig. 3. The measured e.m.f. are then integrated to

obtained the flux linkage (λ) in order to compute the magnetizing inductance using the expression in (2) [9].

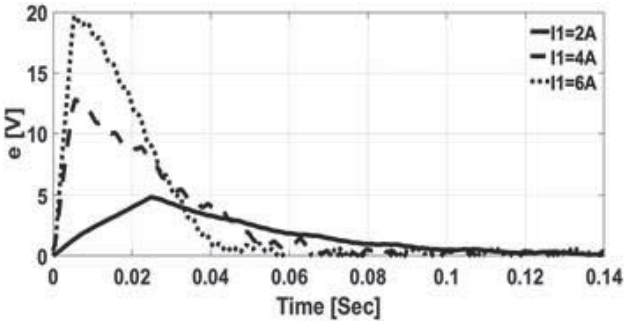

Fig. 3. Measured e.m.f.

$$X_m = (3\lambda / I_1)2\pi f \quad (2)$$

The plot of magnetizing current versus d.c. input current is illustrated in Fig. 4 (marked by the dotted line). It can be seen that the obtained mutual reactance declines in nonlinear manner as the applied d.c. input current is increased. The saturation degree is increased in correlation with an increasing in the input current beyond its rated value (2.8A). The value of mutual reactance can be expressed using the saturation function with the given coefficients as shown in Fig. 4.

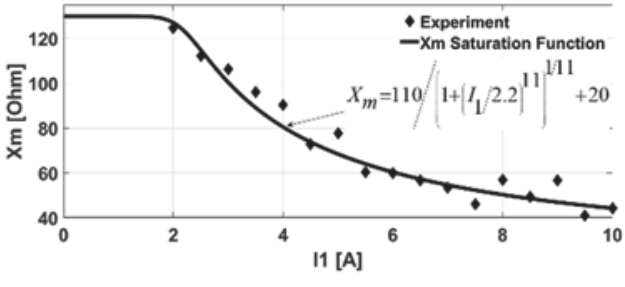

Fig. 4. Mutual reactance at different levels of current .

Next, the rotor leakage reactance can be measured at different levels of currents by using the locked- rotor method commonly found in the conventional text book [6] . The plot of obtained leakage reactance is displayed in Fig. 5. It is evident that the value of this reactance is varied with increasing current in the similar manner as found in the case of mutual reactance. Finally, the rotor resistance can be also determined using the locked-rotor method. The frequency of the supply voltage feeding the stator of the test motor is adjusted from 50Hz to 0Hz. The plot of

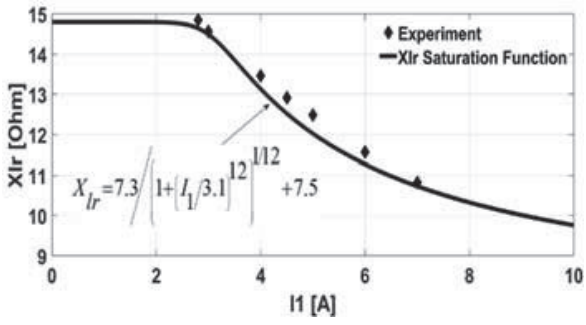

Fig.5. Rotor leakage reactance at different levels of current

obtained resistance is shown in Fig. 6. It can be seen that the resistance of rotor winding is certainly changed due to a variation in the operating frequency. So, this change must be taken into consideration for the torque-speed curve calculation since the operating frequency of the rotor circuit is reduced in corresponding to a decreasing in speed during braking.

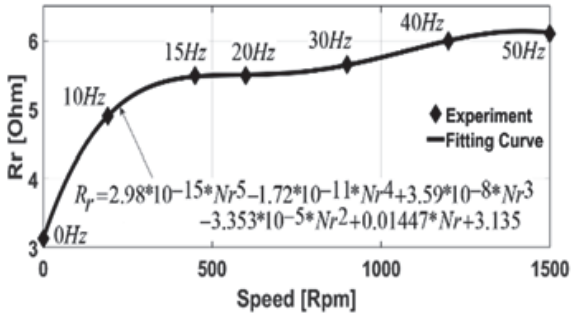

Fig.6. Rotor resistance at different operating speeds

5. Discussion and result

This section presents comparative results between the measurement and calculation of the speed-torque curves at different levels of d.c. current injections. The torque-speed curve of test motor in Fig. 2 is measured once at a time when the d.c. currents of 4A, 6A, 8A, are applied. It should be noted that three different connections of the stator windings, namely configurations 1, 2 and 3, respectively, are carried out as shown in Fig. 2a. The 1st configuration simply considers only one winding while the others take two or three windings in series connection. If

two or three windings schemes are used, the vector sum of the stator d.c. current IDC must be done in order to get the correct value of the resultant stator current I1 where is required for torque-speed-curve computation using (1). Using the tested parameters as obtained from the previous section, the computed braking torque curves against speed are given in Fig.7. For making a comparison, the torque curves of the tested motor are also measured (solid lines). It can be seen that the braking torques increase until they reach the highest torque (maximum braking torque) at the low speed region. Then, the braking torque suddenly falls as the speed drops further. It is noted that the measured and calculated torque curves obtained from the three configurations at different levels of injected currents are seem to be in calculation and measurement are slightly shown particularly around the speed at which the maximum braking torques occur.

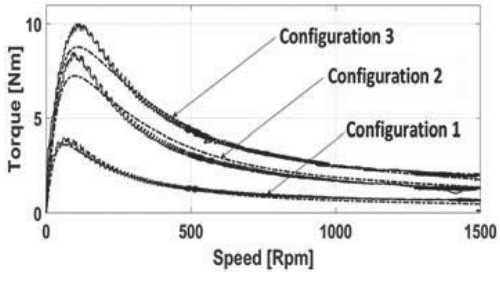

7a Torque curves at 4A

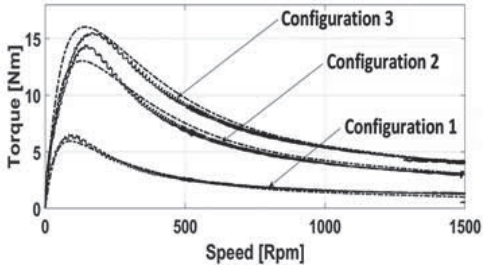

7b Torque curves at 6A

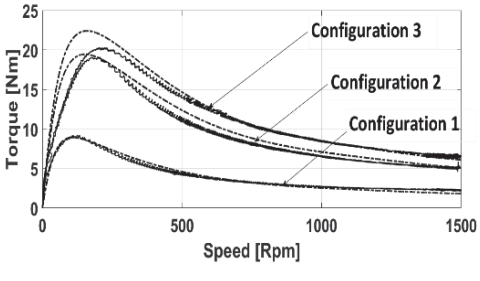

7c Torque curves at 8A

Fig. 7. Different torque-speed curves

6. Conclusion

This paper demonstrates the calculation of braking torque curves of induction motor under the d.c. current injection. The nonlinear saturations of mutual and rotor-leakage reactances as well as the slip-dependent resistance in the rotor circuit are taken in account. It is shown from the presented results that the accurate braking torque-speed curves of induction motor can be obtained by incorporating both saturation and slip-dependent effects. Good agreements between the measured and calculated torque curves are well accepted in satisfactory manner. The well-computed torque curve could be further used for analyzing the braking performance of the induction motors under d.c. current injection.

References

[1] C.Somer, C.Moussa, K.A.Haddad, (2015). Emergency dc injection braking system. IEEE International Conference on Industrial Technology (ICIT), 726-730.

[2] P. L. Rongmei, S.L.Shimi, S. Chatterji, V.K.Sharma, (2012). A novel fast braking system for induction motor. International Journal of Engineering and Innovative Technology (IJEIT), 65-69.

[3] R.Berry, P.Chadwick, (2019). Electrical Trade Practices 2nd edition. Australia: Cengage Learning Australia.

[4] M.G. Say, (1949). Design of Alternating Current Machines. London: Pitman.

[5] D.Harrison, (1956). The dynamic braking of induction motors . IET, 121-129.

[6] P.C. Sen, (2014). Principles of Electrical Machines and Power Electronic. 3rd ed. NJ: Wiley.

[7] J. Pedra, I.Candela, A.Barrera, (2009). Saturation model for squirrel cage induction motor. Electric Power Systems Research, 1054-1061.

[8] A. Boglietti, A.Cavagnino, L.Ferraris, M. Lazzari, (2010). Skin effect experimental validations of induction motor squirrel cage parameters. The International Journal for Computation and Mathematics in Electrical and Electronic Engineering, 1257-1265.

[10] A.V.Stankovic, E.L.Benedict, V.John, T.A. Lipo, (2003). A novel method for measuring induction machine. IEEE Transaction on